

CONF. 780609--1

LA-UR-77-2754

**TITLE:** STRUCTURAL DESIGN FOR A 10-GWh SMES VACUUM VESSEL

**AUTHOR(S):** Joel G. Bennett  
Charles A. Anderson

**MASTER**

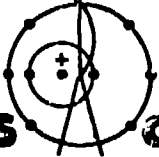
**SUBMITTED TO:** 1978 ASME/CSME Pressure Vessels and Piping  
Conference with Nuclear and Materials Div.  
June 25-29, 1978  
Montreal, Canada

**NOTICE**  
This report was prepared as an account of work sponsored by the United States Government. Neither the United States nor the United States Department of Energy, nor any of their employees, nor any of their contractors, subcontractors, or their employees, makes any warranty, express or implied, or assumes any legal liability or responsibility for the accuracy, completeness or usefulness of any information, apparatus, product or process disclosed, or represents that its use would not infringe privately owned rights.

By acceptance of this article for publication, the publisher recognizes the Government's (license) rights in any copyright and the Government and its authorized representatives have unrestricted right to reproduce in whole or in part said article under any copyright secured by the publisher.

The Los Alamos Scientific Laboratory requests that the publisher identify this article as work performed under the auspices of the USERDA.

... NOT AVAILABLE. It  
... to the best available  
... the broadest possible avail-  
ability.

  
**los alamos**  
**scientific laboratory**  
of the University of California  
LOS ALAMOS, NEW MEXICO 87545

An Affirmative Action/Equal Opportunity Employer

DISTRIBUTION OF THIS

# STRUCTURAL DESIGN FOR A 10-GWh SMES VACUUM VESSEL

by

Joel G. Bennett\* and Charles A. Anderson\*\*

## ABSTRACT

An approximate solution to the problem of the non-linear elastic deformation of a periodically point-supported cylindrical shell is obtained. This solution is used to investigate the structural design of the vacuum vessel for the large underground SMES concept. Vacuum vessel designs are evaluated by varying such parameters as shell thickness, support spacing, material properties and physical configuration to keep the amount of material used and construction cost to a minimum.

---

## I. INTRODUCTION

The conceptual design and feasibility studies for superconducting magnetic energy storage (SMES) facilities indicate that the energy storage cost rates decrease rapidly with increasing facility capacity.<sup>1,2</sup> Thus, present studies have focused attention on 10-GWh capacity plants.<sup>3,4,5</sup> In the large underground SMES concept that will be considered here, the proposed vessel is about 100 m in height and about 300 m in diameter. The large dimensions of the

---

\* Staff Member, Group Q-13, Los Alamos Scientific Laboratory, Box 1663, Los Alamos, New Mexico 87545

\*\* Staff Member, Group Q-13, Los Alamos Scientific Laboratory, Box 1663, Los Alamos, New Mexico 87545; Member ASME.

vessel make it imperative that the material costs be minimized. Because the total area of the outer vacuum vessel is  $94,000 \text{ m}^2$ , significant cost savings can be effected by relatively small decreases in vessel wall thickness that could be brought about in an optimized structural design.

The main structural problem that will be formulated will be that of the deformation of a point-supported shell liner under an external pressure of one atmosphere as shown schematically in Fig. 1a; because of the large support spacing and thinness of the shell, the deflections will be large with respect to the thickness. Hence, even though the material remains linearly elastic, the problem is basically one of nonlinear deformation. The formulation will include the kinematics necessary to solve for the entire load displacement history and thus to account for stability of the shell. The primary quantities of interest are the maximum displacement and maximum stresses in the shell. This problem can be specialized to include Fig. 1b and 1c by allowing the axial support spacing to become very small, and adjusting other solution parameters appropriately.

In prior investigations, Kicker<sup>6</sup> studied the problem of preventing snap-through buckling of point-supported, concrete-encased liner-shells by specializing Fig. 1a to point supported rings and axisymmetric cylinders. For the problem considered here, "snap-through" type deformation is assumed to occur a priori. In reality, for the radius of curvature of the 10-GWh vessel and for large support spacings, the deformation is very much like that of a continuous point-supported plate.

The advantage of formulating the problem from the point of view of the unstrained surface being a cylinder is the applicability of the solution to other configurations such as those shown in Fig. 1b and 1c and to smaller vessels. Various extensions of the method employed in Ref. 6 have been

carried out<sup>7,8,9</sup> and these are summarized in Ref. 10. In Ref. 10, Moon and Kicker also extended the study of concrete encased linear shells to include closely spaced anchors; the plastic design method was employed. In these cases, the structural members were idealized as rings, beams or axisymmetric shells.

The economic and feasibility study by the University of Wisconsin<sup>2,3</sup> gives cost estimates for the 10-GWh concept based on an assumed vessel thickness and material, but no design or structural study basis for the thickness or material is indicated.

## II. ANALYTICAL MODEL FORMULATION

### A. Strain-Displacement Relations

Beginning with the large strain-displacement relations from continuum mechanics as expressed in cylindrical coordinates and applying the same assumptions attributable to von Karman<sup>11</sup> for the large deflection of plates, the total strain displacement equations for a cylindrical surface can be derived as

$$\begin{aligned}\epsilon_x &= \frac{\partial u}{\partial x} - z \left( \frac{\partial^2 w}{\partial x^2} \right) + \frac{1}{2} \left( \frac{\partial w}{\partial x} \right)^2 \\ \epsilon_\theta &= \frac{1}{R} \left( \frac{\partial v}{\partial \theta} + w \right) - \frac{z}{R^2} \left( \frac{\partial^2 w}{\partial \theta^2} \right) + \frac{1}{2R^2} \left( \frac{\partial w}{\partial \theta} \right)^2 \\ \gamma_{x\theta} &= \frac{1}{R} \frac{\partial u}{\partial \theta} + \frac{\partial v}{\partial x} - \frac{2z}{R} \left( \frac{\partial^2 w}{\partial x \partial \theta} \right) + \frac{1}{R} \left( \frac{\partial w}{\partial x} \right) \left( \frac{\partial w}{\partial \theta} \right)\end{aligned}\quad (1)$$

where,

x ... the axial coordinate

$\theta$  ... the circumferential coordinate

z ... thickness coordinate relative to the middle surface

u ... the axial displacement

v ... the circumferential displacement

w ... the radial displacement of the middle surface

R ... radius of the undeformed middle surface

$\epsilon_x$  ... axial strain

$\epsilon_\theta$  ... circumferential strain

$\gamma_{x\theta}$  ... in-plane shear strain.

As pointed out in Ref. 11, this theory keeps the first order nonlinear terms in the gradients of w and the expression "large deflections" refers to the fact that displacement w and its gradients are no longer small relative to the shell thickness.

### B. Hooke's Law and Strain Energy

To minimize costs, the vacuum vessel liner will be made from a conventional structural metal such as stainless steel or aluminum and we wish to keep the design elastic. Thus, we describe the stress-strain relations with Hooke's Law. Beginning with the full three-dimensional form, including uniform thermal expansion, and assuming a thin shell and thus a state of two-dimensional stress, these relations become

$$\begin{aligned}\sigma_x &= \frac{E}{1-\nu^2} (\epsilon_x + \nu\epsilon_\theta) - \frac{E\alpha\Delta T}{1-\nu} \\ \sigma_\theta &= \frac{E}{1-\nu^2} (\epsilon_\theta + \nu\epsilon_x) - \frac{E\alpha\Delta T}{1-\nu}\end{aligned}\tag{2}$$

$$\tau_{x\theta} = G\gamma_{x\theta}$$

where,

$\sigma_x$  ... the axial normal stress

$\sigma_\theta$  ... the hoop normal stress

$\tau_{x\theta}$  ... the in-plane shearing stress

E ... Young's modulus of elasticity

$\nu$  ... Poisson's ratio

G ... Shear modulus of elasticity

$\alpha$  ... the coefficient of thermal expansion

$\Delta T$  ... the change in temperature from the reference temperature

We will enforce equilibrium by minimization of the shell potential energy. Following a standard procedure we define the expression for the strain energy density function,  $\bar{U}$ , as

$$d\bar{U} = \frac{1}{2} \sigma_{ij} d\epsilon_{ij} \quad (\text{sum on } i, j)$$

Substitute into this definition the expressions for stresses from Eq. 2, and assume intermediate states of strain are proportional to the final state. Next, integrate from the unstrained state to the final strain state, and the expression for the strain energy per unit shell volume is

$$\bar{U} = \frac{E}{2(1-\nu^2)} \left( \epsilon_x^2 + 2\nu\epsilon_x\epsilon_\theta + \epsilon_\theta^2 \right) - \frac{E\alpha\Delta T}{1-\nu} (\epsilon_\theta + \epsilon_x) + \frac{G\gamma_{x\theta}^2}{2} \quad (3)$$

The total strain energy is that given by  $U = \int_V \bar{U} dV$ .

Substituting the strain displacement relations into Eq. 3 and carrying out the integration over the shell thickness, we arrive at the expression for the strain energy for the shell as

$$\begin{aligned} U = \iint \frac{1}{2} \left\{ \left[ \left( u_{,x} + \frac{1}{2} w_{,x}^2 \right)^2 + \frac{1}{R^2} \left( v_{,\theta} + w \right)^2 \right. \right. \\ + \frac{1}{R^3} \left( v_{,\theta} w_{,\theta}^2 + w w_{,\theta}^2 \right) + \frac{1}{4R^4} w_{,\theta}^4 + \frac{\nu}{R} \left( 2u_{,x} v_{,\theta} + 2u_{,x} w \right. \\ \left. \left. + \frac{1}{R} u_{,x} w_{,\theta}^2 + w_{,x}^2 v_{,\theta} + w_{,x}^2 w + \frac{1}{2R} w_{,x}^2 w_{,\theta}^2 \right) \right. \\ \left. - 2(1+\nu)\alpha\Delta T \left( \frac{1}{R} v_{,\theta} + \frac{w}{R} + \frac{1}{2R^2} w_{,\theta}^2 + u_{,x} + \frac{1}{2} w_{,x}^2 \right) \right\} \end{aligned} \quad (4)$$

$$\begin{aligned}
 & + D \left( w_{,xx}^2 + \frac{1}{R^4} w_{,\theta\theta}^2 + \frac{2\nu}{R^2} w_{,xx} w_{,\theta\theta} \right) \\
 & + Gh \left( \frac{1}{R} u_{,\theta} + v_{,x} + \frac{1}{R} w_{,x} w_{,\theta} \right)^2 \\
 & + \left. \frac{Gh^3}{3R^2} w_{,x\theta}^2 \right\} R d\theta dx
 \end{aligned}$$

The comma notation refers to partial differentiation of the dependent variable with respect to the coordinates following the comma, and we have, as is the custom, defined the membrane and flexural shell stiffnesses as

$$\kappa = \frac{Eh}{1-\nu^2} \quad D = \frac{Eh^3}{12(1-\nu^2)}$$

with  $h$  being the shell thickness.

### C. Variational Method

Having an expression for the strain energy, we can treat the functional Eq. 4 by a number of variational methods. The one we will use is basically a modified Ritz method, as described in Ref. 12, and outlined below.

1. Using the functional Eq. 4, we derive the equilibrium equations as the resulting Euler equations obtained by minimizing Eq. 4 with respect to the displacements.

2. Defining the membrane equations of equilibrium as those expressing equilibrium in the  $u$  and  $v$  directions, we solve these differential equations in terms of an assumed solution in  $w$ .

3. Substitute the resulting expressions for the displacements  $u$  and  $v$  and the assumed displacement function for  $w$  into Eq. 4 and carry out the indicated integration. The resulting expression for  $U$  involves the unknown amplitudes of the  $w$  displacement function.

4. Form the total potential energy,  $\Pi$ , by subtracting from the strain energy the work  $W$  done by the loading function, i.e.,  $\Pi = U - W$ .

5. We now require the total potential energy  $\Pi$  to be a minimum with respect to the unknown amplitudes of the assumed displacement function. As described in Ref. 12, for quadratic functionals, the resulting Euler equations will be linear algebraic equations. Here, the functional (Eq. 4) is 4th order in  $w$  and the resulting algebraic equations will be cubic in the unknown amplitudes. We can solve these equations numerically to obtain the solutions for displacements and stresses. Parameter studies then allow the vessel design to be carried out.

#### D. Assumed Displacement Function

Figure 2 shows the coordinate system used to describe the shell and the shell deformation pattern. We assume the shell is isothermal and that the displacement  $w$  can be described by a series of orthogonal functions of the form

$$w = a_0 + \sum_{m=1}^{\infty} a_{mx} \cos mp_x + \sum_{n=1}^{\infty} a_{n\theta} \cos nq\theta \quad (5)$$

where

$$p = \frac{2\pi}{b} \quad \text{and} \quad q = \frac{2\pi}{R\theta_0} = \frac{2\pi}{a}$$

The condition  $w = 0$  at all supports gives the auxiliary equation that

$$a_0 = - \sum_{n,m} (a_{mx} + a_{n\theta}) .$$

With this auxiliary equation, the assumed displacement function satisfies all boundary conditions of zero slopes and displacements at the support points for a continuous shell. We note, however, that in using this displacement

function, we have made one additional assumption, that is, that  $\frac{\partial^2 w}{\partial x \partial \theta} = 0$ , which implies that the variation of the in-plane shearing strain through the thickness of the shell is negligible (see Eq. 1). For a thin shell of large curvature and under the pressure loading of interest, this assumption should be a reasonable one. In a later section we compare the result of this solution with a solution given from the general nonlinear finite element code NONSAP.<sup>14</sup>

For practical purposes, the displacement function  $w$  must be truncated; for linear small displacement theory one term is adequate, such as is done for beam columns in Ref. 13. Reference 6 apparently obtains good results from a single term expansion for the ring and axisymmetric cylinder problems considered there. Reference 10 also uses a single term. One term in each series, however, does not allow the decreased curvature (and consequent bending moment) at the supports to be adequately described for widely spaced supports. Physically, behavior near the support should be dominated by bending while in the center of the support pattern, membrane action should dominate. At least two terms in both series of Eq. 5 are required to allow the minimization procedure to represent this behavior.

Specialization of the general solution to two terms in each series, yields four coupled cubic equations for the unknowns  $a_{1x}$ ,  $a_{2x}$ ,  $a_{1\theta}$ , and  $a_{2\theta}$ , that are given in Appendix A. A direct iteration procedure was used to solve for these coefficients.

### III. APPLICATIONS

#### A. Elastic Design of a Periodically-Supported Shell

The first configuration studied with this solution is the one of Fig. 1a. In this design concept, the shell is visualized as a continuous structure made from welded plates and anchored to the rock cavity by a regular array of rock anchors. The anchor points are also potential magnet structural support points.

In an integrated design, the rock anchor may become an integral part of the vessel wall support and can be extended into a strut for the magnet support.

Several questions of interest are as follows:

1. How does the periodic support spacing affect the maximum stress and the maximum displacement?
2. How do the material properties affect the maximum stress?
3. How does the thickness of the shell affect the maximum stress?

This initial study assumes that the vessel walls will be constructed of common structural materials. A-304 annealed stainless steel and 5083-H38 aluminum properties were initially used. Tables I and II summarize the parameter studies for these two materials and Fig. 3 shows typical pressure-displacement curves for a periodic support spacing array of 2 m and stainless steel of different thicknesses. Also shown on this figure are the results of an elastic analysis using the finite element code NONSAP<sup>14</sup> for the case of shell radius  $R = 150$  m and thickness of 10 mm. (The mesh used for this study is described in a later section.) The agreement between the two solutions is very good with the analytical solution predicting a maximum center displacement of  $w = 43.5$  mm and NONSAP predicting a center displacement of  $w = 46.8$  mm. The stresses were not directly compared at specific points but they agree in magnitude very well. The conclusion is that under this loading condition, the assumption of negligible variation through the thickness of the in-plane shear is justified.

Examination of Table I reveals that it will not be economically feasible to specify a vessel design from stainless steel that remains entirely elastic in the annealed condition. Figure 4 illustrates this point graphically. Using a linear extrapolation in Fig. 4 (and a value of 207 MPa for the yield strength) the minimum thickness of A-304 stainless steel for a potentially

totally elastic design (according to Tresca yield criteria) is about 17 mm with a support spacing on 1 m centers. Even for higher yield strengths of stainless steel, thickness reductions below 1 cm lead to very high values of maximum stress.

On the other hand, (using a value of 385 MPa as the yield strength of 5083 aluminum in the H38 condition) Table II and Fig. 4 reveal that almost all values given for aluminum are within the elastic limit.

Closer examination of Tables I and II reveal two further points of interest. First, the bending stresses at the support points are more severe for the case of the stiffer material. Second, the nonlinearities that arise because of the large deformations show up as apparent anomalies in the maximum predicted stresses caused primarily by shell bending. In particular, reading across the tables, the trends for the two materials are clearly different. The membrane stresses, however, do show the same trends.

The effect of having a more flexible material apparently is to reduce the overall stress level by transmitting more of the load into the supports. For example, for the case of the support spacing being 2 m on center and a shell thickness of 10 mm, the anchor reaction force for an aluminum vessel is 11.7 kN as compared to that for a stainless steel vessel of 10.5 kN.

Figure 5 illustrates this effect graphically and can be used to examine other candidate materials. It is readily seen from Fig. 5 that the best materials for this application are those with a relatively large ratio of tensile yield strength to elastic modulus.

#### B. Elastic-Plastic Design of a Periodically-Supported Shell

Examination of Table I reveals that only in the locations for which the bending stresses are maximum is the elastic limit for the materials exceeded. For this reason, the possibility of taking advantage of the residual strength

available in an elastic plastic design has been briefly investigated. The general nonlinear finite element code NONSAP<sup>14</sup> was used for this study.

Figure 6 shows the three-dimensional mesh and boundary conditions used to model the shell for the 2 x 2 m support spacing. This mesh consists of 16, 16-node solid elements and a total of 130 nodes. The NONSAP code allows a von Mises' yield condition with kinematic hardening for the three-dimensional elements to model the plastic effects. The initial yield stress was set at 207 MPa and a 1% strain hardening modulus was used to model the properties of annealed stainless A-304. The predicted pressure-displacement curve for the center of the support pattern for the elastic-plastic case is also shown on Fig. 3. The approximate extent of the plastic zone predicted in the analysis is shown in Fig. 7. Although the plastic zone extends over about 25% of the mesh, the predicted strains are in general reasonable except near the load singularity at node 130. In this regard, it must be pointed out that at all the supports, the load transmitted to the rock must be spread out over a finite area.

The purpose of this calculation is to demonstrate that a candidate material should not be excluded based only on the stresses exceeding the yield criterion, and that the elastic-plastic design potential exists. In this particular calculation the plastic zone is probably too extensive for a reasonable design, but further investigations in this area will undoubtedly prove fruitful.

### C. Structural Member and Shell Combination Design

By allowing the axial spacing to approach zero, adjusting the radius of curvature, and reversing the sign of the pressure loading, the solution for the point supported shell degenerates to that of Fig. 2, b and c. The I-Beams are, of course, symbolic of some type of structural member that can be used to anchor the vessel to the rock cavity. The design concept is a series

of shells or plates with clamped ( $w = 0, \frac{\partial w}{\partial \theta} = 0$ ) axial boundaries. Large elastic deformations of the shell are allowed however.

A number of computer runs were made to assess the design potential of this configuration. Figure 8 gives the definition of the various geometric parameters. The radius of curvature  $R$ , shell arc length  $S$ , and the rise  $D$ , are related by the transcendental equation.

$$R \left( 1 - \cos \frac{S}{2R} \right) = D.$$

The chord length,  $C$ , which determines the number of structural supports needed, is given by  $C = R \sin \frac{\theta}{2}$  where  $S = R\theta$ .

This concept was studied parametrically and the results are reported in Ref. 15.

Figure 9 gives a typical result and shows the effect of varying the initial unstrained rise of the shell, (and thus the radius of curvature,  $R$ ) on the maximum stress. As can be seen, the flat plate configuration obtained from the  $D = 0$  extrapolation is not the worst case. The nonlinearities that arise from the combined bending and large deformations illustrate that a definite maximum occurs in the maximum stress as a function of the unstrained shell curvature.

Also, Fig. 9 shows the effect of the two different material properties, and defines the extent of the nonlinear region for this design concept. This curve illustrates that for rises of  $D \approx 1$  m and greater, the nonlinearities due to the large displacements become less pronounced. The stresses are predominantly membrane stresses and the effect of having a more flexible material disappears as the rise increases.

#### IV. SUMMARY

The main result of this study is that a large radius vacuum vessel can

be designed to minimize material by using optimally spaced point supports. Also, the study indicates that given two materials with the same yield strengths, the lower modulus material will lead to a thinner vacuum vessel wall.

The two term deformation shape function appeared to give sufficiently accurate results for the vacuum vessel design. For instance, the one and two term solutions gave about 12 percent difference in values for the maximum displacement. A study of the coefficients in the equations for the one, two, and a three-term approximation indicate that the addition of more terms in the solution will serve only to correct slightly the two-term solution. Since the solution is only approximate because of the neglect of the shear variation through the shell thickness, the further addition of terms will probably not add any accuracy to the solutions as given.

## APPENDIX A

## BASIC EQUATIONS

The general equations resulting from carrying out the steps described in Section D for the assumed displacement function of Eq. 5 have been obtained. These equations were then specialized to a one-term approximation that results in two simultaneous cubic equations for  $a_{1x}$  and  $a_{1\theta}$ , and to a two-term approximation resulting in four simultaneous cubic equations for  $a_{1x}$ ,  $a_{2x}$ ,  $a_{1\theta}$ , and  $a_{2\theta}$ . These latter four equations are recorded below:

$$\begin{aligned}
& \frac{\kappa p^4}{2} a_{1x}^3 - \frac{3\nu\kappa p^2}{2R} a_{1x}^2 + \left[ \kappa \left( \frac{3-\nu^2}{R^2} \right) - \kappa(1+\nu)\alpha\Delta T p^2 + Dp^4 \right] a_{1x} \\
& + \left[ \kappa \left( \frac{p^2}{2} f_{11}^2 + \frac{q^2}{2} g_{11}^2 + \nu p q f_{11} g_{11} + \frac{\nu p^2 q^2}{4} \right) + \frac{Gh}{2} C_{11}^2 \right] a_{1\theta}^2 a_{1x} \\
& + \left[ \kappa \left( \frac{p^2}{2} f_{12}^2 + 2q^2 g_{12}^2 + 2\nu p q f_{12} g_{12} + \nu p^2 q^2 \right) + \frac{Gh}{2} C_{12}^2 \right] a_{2\theta}^2 a_{1x} \\
& + \kappa \left[ 2p^4 a_{2x}^2 - \frac{3\nu p^2}{2R} a_{2x} - \frac{\nu p^2}{R} (a_{1\theta} + a_{2\theta}) \right] a_{1x} \\
& + \kappa \left[ \frac{2}{R^2} (a_{2x} + a_{1\theta} + a_{2\theta}) - \frac{q^2}{2R} a_{1\theta}^2 - \frac{2q^2}{R} a_{2\theta}^2 + \frac{2(1+\nu)\alpha\Delta T}{R} \right] \\
& - 2P_r = 0
\end{aligned} \tag{A1}$$

$$\begin{aligned}
& 8\kappa p^4 a_{2x}^3 - \frac{6\nu\kappa p^2}{R} a_{2x}^2 + \left[ \frac{5-\nu^2}{R^2} \kappa - 4\kappa(1+\nu)\alpha\Delta T p^2 + 16Dp^4 \right] a_{2x} \\
& + \left[ \kappa \left( 2p^2 f_{21}^2 + \frac{q^2}{2} g_{21}^2 + 2\nu p q f_{21} g_{21} + \nu p^2 q^2 \right) + \frac{Gh}{2} C_{21}^2 \right] a_{1\theta}^2 a_{2x} \\
& + \left[ 2\kappa \left( p^2 f_{22}^2 + q^2 g_{22}^2 + 2\nu p q f_{22} g_{22} + 2\nu p^2 q^2 \right) + \frac{Gh}{2} C_{22}^2 \right] a_{2\theta}^2 a_{2x}
\end{aligned}$$

$$\begin{aligned}
& + 2\kappa \left[ p^4 a_{1x}^2 - \frac{2vp^2}{R} (a_{1x} + a_{1\theta} + a_{2\theta}) \right] a_{2x} \\
& + \kappa \left[ \frac{2}{R^2} (a_{1x} + a_{1\theta} + a_{2\theta}) - \frac{q^2}{2R} a_{1\theta}^2 - \frac{2q^2}{R} a_{2\theta}^2 + \frac{vp^2}{R} a_{1x}^2 \right. \\
& \left. + \frac{2(1+\nu)\alpha\Delta T}{R} \right] - 2P_r = 0 \quad . \quad (A2)
\end{aligned}$$

$$\begin{aligned}
& \frac{\kappa q^4}{2} a_{1\theta}^3 - \frac{3\kappa q^4}{2R} a_{1\theta}^2 + \left[ \frac{2\kappa}{R^2} - \kappa(1+\nu)\alpha\Delta T q^2 + Dq^4 \right] a_{1\theta} \\
& + \left[ \kappa \left( \frac{p^2}{2} f_{11}^2 + \frac{q^2}{2} g_{11}^2 + v p q f_{11} g_{11} + \frac{vp^2 q^2}{4} \right) + \frac{Gh}{2} C_{11}^2 \right] a_{1x}^2 a_{1\theta} \\
& + \left[ \kappa \left( 2p^2 f_{21}^2 + \frac{q^2}{2} g_{21}^2 + 2v p q f_{21} g_{21} + vp^2 q^2 \right) + \frac{Gh}{2} C_{21}^2 \right] a_{2x}^2 a_{1\theta} \\
& + \kappa \left[ 2q^4 a_{2\theta}^2 - \frac{3q^2}{2R} a_{2\theta} - \frac{q^2}{R} (a_{1x} + a_{2x}) \right] a_{1\theta} \\
& + \kappa \left[ \frac{2}{R^2} (a_{1x} + a_{2x} + a_{2\theta}) - \frac{vp^2}{2R} a_{1x}^2 - \frac{2vp^2}{R} a_{2x}^2 \right. \\
& \left. + \frac{2(1+\nu)\alpha\Delta T}{R} \right] - 2P_r = 0 \quad . \quad (A3)
\end{aligned}$$

$$\begin{aligned}
& 8\kappa q^4 a_{2\theta}^3 - \frac{6\kappa q^2}{R} a_{2\theta}^2 + \left[ \frac{2\kappa}{R^2} - 4\kappa(1+\nu)\alpha\Delta T q^2 + 16Dq^4 \right] a_{2\theta} \\
& + \left[ \kappa \left( \frac{p^2}{2} f_{12}^2 + 2q^2 g_{12}^2 + 2v p q f_{12} g_{12} + vp^2 q^2 \right) + \frac{Gh}{2} C_{12}^2 \right] a_{1x}^2 a_{2\theta} \\
& + \left[ 2\kappa \left( p^2 f_{22}^2 + q^2 g_{22}^2 + 2v p q g_{22} f_{22} + 2vp^2 q^2 \right) + \frac{Gh}{2} C_{22}^2 \right] a_{2x}^2 a_{2\theta} \\
& + \kappa \left[ 2q^4 a_{1\theta}^2 - \frac{4q^2}{R} (a_{1x} + a_{2x} + a_{1\theta}) \right] a_{2\theta} \\
& + \kappa \left[ \frac{2}{R^2} (a_{1x} + a_{2x} + a_{1\theta}) - \frac{vp^2}{2R} a_{1x}^2 - \frac{2vp^2}{R} a_{2x}^2 + \frac{q^2}{R} a_{1\theta}^2 \right.
\end{aligned}$$

$$\left. + \frac{2(1+\nu)\alpha\Delta T}{R} \right] - 2 P_r = 0$$

(A4)

where,

$$f_{ji} = \frac{jp(iq)^2 [(iq)^2 - \nu(jp)^2]}{[(jp)^2 + (iq)^2]^2}$$

$$g_{ji} = \frac{(jp)^2 iq [(jp)^2 - \nu(iq)^2]}{[(jp)^2 + (iq)^2]^2}$$

$$C_{11}^2 = (pq - pg_{11} - qf_{11})^2$$

$$C_{12}^2 = (2pq - pg_{12} - 2f_{12})^2$$

$$C_{21}^2 = (2pq - 2pg_{21} - qf_{21})^2$$

$$C_{22}^2 = 4(2pq - pg_{22} - qf_{22})^2$$

and  $P_r$  is the external pressure loading.

## REFERENCES

1. W. V. Hassenzahl, B. L. Baker, and W. E. Keller, "The Economics of Superconducting Magnetic Energy Storage Systems for Load Leveling," Los Alamos Scientific Laboratory report, LA-5377-MS (August 1973).
2. R. W. Boom, H. A. Peterson, and W. C. Young, Wisconsin Superconductive Energy Storage Project, Vol. I, Engineering Experiment Sta., College of Eng., University of Wisconsin, Madison (July 1974).
3. R. W. Boom, H. A. Peterson, Wisconsin Superconductive Energy Storage System Design, Vol. II, Engineering Experiment Sta., Univ. of Wisconsin, Madison (January 1976).
4. "Reference Designs for 10-MWh and 10-GWh SMES Units," Los Alamos Scientific Laboratory report, to be published.
5. W. E. Keller, "Applications of Superconductivity in Electric Power Systems," presented at the 1976 Frontiers of Power Technology Conference, LA-UR-76-1998, (1976).
6. T. Kicker, "Buckling of a Stud-Supported Thin Cylindrical Liner Shell Encased in Concrete," Nuc. Eng. and Design, 26 (1974) pp. 250-262.
7. T. C. Esselman, Ph.D. Thesis, Case Western Reserve Univ. (June 1973).
8. R. J. Gratzinger, M.S. Thesis, Case Western Reserve Univ. (June 1973).
9. M. J. Schrader, Ph.D. Thesis, Case Western Reserve Univ. (January 1975).
10. Y. I. Moon, T. P. Kicker, "The Plastic Buckling of a Steel Liner Encased in a Concrete Cylinder," Nuc. Eng. and Design, 41 (1977) pp. 281-291.
11. Y. C. Fung, Foundations of Solid Mechanics, Chapter 16, Prentice-Hall, Inc. (1965).
12. I. S. Sokolnikoff, Mathematical Theory of Elasticity, 2nd Ed., Chapter VII, McGraw-Hill (1956).

13. S. P. Timoshenko, J. M. Gere, Theory of Elastic Stability, 2nd Ed., Chapter I, McGraw-Hill (1961).
14. K. J. Bathe, E. L. Wilson, and R. Iding, "NONSAP - A Structural Analysis Program for Static and Dynamic Response of Nonlinear Systems," Univ. of California report, USCESM 74-3 (February 1974).
15. J. G. Bennett, C. A. Anderson, "Structural Design for a 10-GWh SMES Vacuum Vessel," Los Alamos Scientific Laboratory report, to be published.

## FIGURE CAPTIONS

Figure 1. Vacuum vessel wall design concepts.

(a) Periodically point-supported cylindrical shell concept.

(b) Structural member and cylindrical shell combination.

(c) Point supported welded cylindrical shell.

Figure 2. Assumed shell displacement pattern and coordinate system used to describe the shell under an external pressure loading.

Figure 3. Center of support array amplitude vs pressure for a stainless steel vessel for 2 x 2 m supports.

Figure 4. Maximum predicted "elastic" hoop stress vs shell thickness as a function of support spacing.

Figure 5. Effect of the modulus of elasticity on the maximum stress for the continuous shell concept.

Figure 6. Finite element mesh used in NONSAP investigation.

Figure 7. Extent of plastic zone from the finite element investigation.

Figure 8. Parameter definition and geometry of the shell-structural member combination concept.

Figure 9. Effect of the unstrained rise,  $D$ , on the maximum stress for a support spacing of  $S = 10$  m as a function of the material properties.

TABLE I

## SUMMARY OF PARAMETER STUDIES FOR STAINLESS STEEL

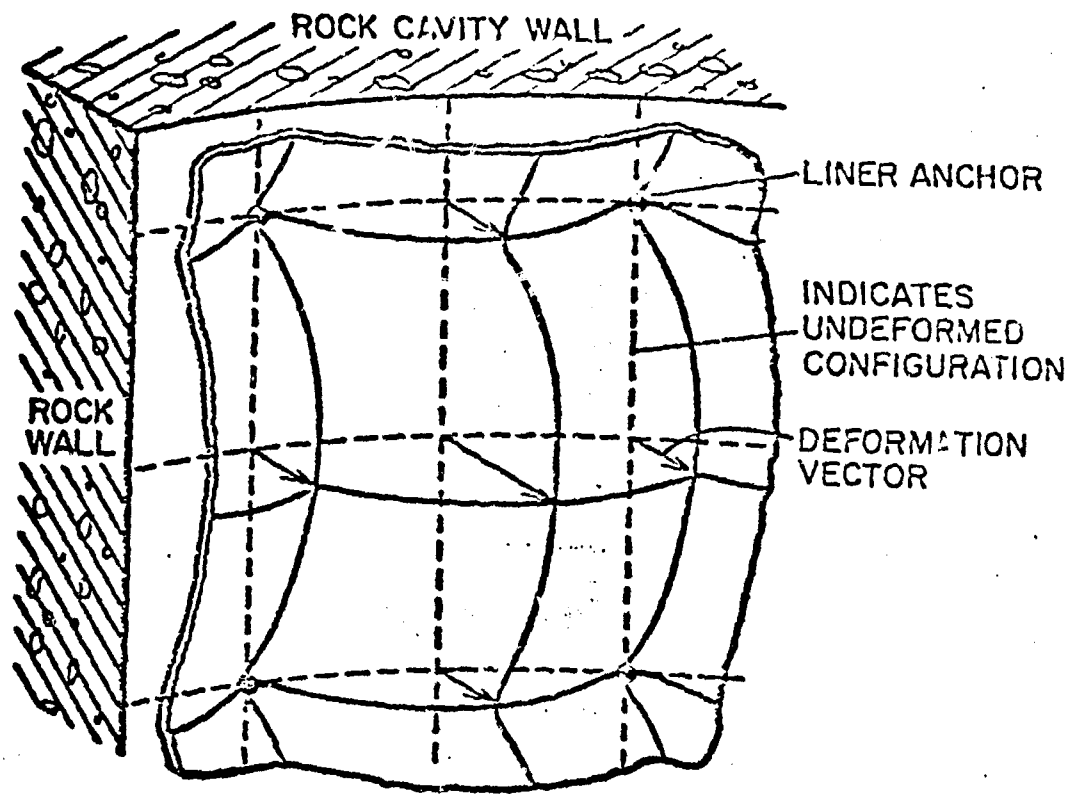
Support Spacing	Elastic Stress Component *Location	Thickness (2t)	Axial Stress MPa(ksi)				Hoop Stress MPa(ksi)				Thinnest Shell Maximum w Displacement at Center of Supports m (inches)
			1.5	1.0	0.5	0.25	1.5	1.0	0.5	0.25	
2 x 2 m	1		409 (59)	455 (66)	516 (75)	-	413 (60)	458 (66)	518 (75)	-	0.545 x 10 <sup>-1</sup> (2.15)
	2		-182 (-26)	-86 (-12)	139 (20)	-	-188 (-27)	-89 (-13)	137 (20)	-	
	3		-7 (-1)	81 (12)	186 (27)	-	-50 (-7)	35 (5)	136 (20)	-	
	4		168 (24)	151 (22)	194 (28)	-	153 (22)	127 (18)	155 (22)	-	
1.5 x 1.5 m	1		353 (51)	425 (62)	486 (71)	-	356 (52)	428 (62)	488 (71)	-	0.368 x 10 <sup>-1</sup> (1.45)
	2		-216 (-31)	-157 (-23)	41 (6)	-	-223 (-32)	-161 (-23)	40 (6)	-	
	3		-72 (-10)	23 (3)	146 (21)	-	-98 (-14)	-9 (-1)	111 (16)	-	
	4		177 (26)	158 (23)	165 (24)	-	169 (25)	145 (21)	140 (20)	-	
1 x 1 m	1		-	352 (51)	453 (66)	513 (74)	-	354 (51)	455 (66)	514 (75)	0.265 x 10 <sup>-1</sup> (1.05)
	2		-	-214 (-31)	-83 (-12)	140 (20)	-	-219 (-32)	-86 (-12)	138 (20)	
	3		-	-70 (-10)	84 (12)	187 (27)	-	-87 (-13)	62 (9)	163 (24)	
	4		-	175 (25)	147 (21)	191 (28)	-	169 (25)	134 (19)	172 (25)	

TABLE II

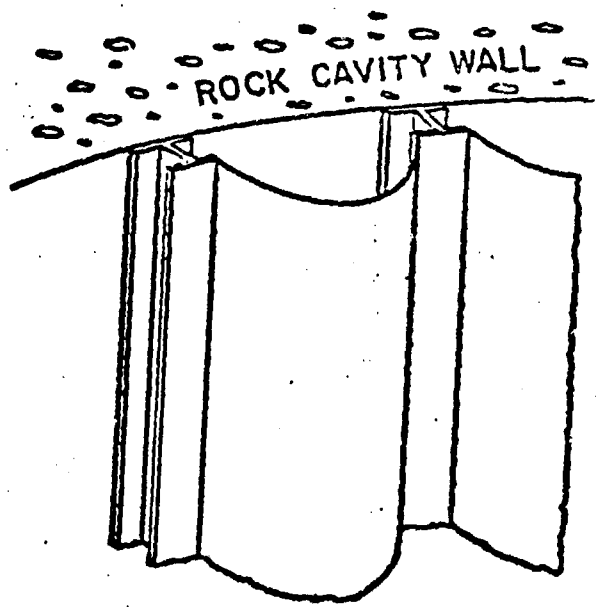
## SUMMARY OF PARAMETER STUDIES FOR ALUMINUM

Support Spacing	Elastic Stress Component *Location	Thickness (cm)	Axial Stress MPa				Hoop Stress MPa				Thinnest Shell Maximum w Displacement at Center of Supports m (inches)
			1.5	1.0	0.5	0.25	1.5	1.0	0.5	0.25	
2 x 2 m	1		268 (39)	286 (41)	331 (48)	434 (63)	270 (39)	288 (42)	331 (48)	434 (63)	0.75 x 10 <sup>-1</sup> (2.97)
	2		-80 (-12)	-10 (-1)	134 (19)	309 (45)	-82 (-12)	-11 (-2)	133 (19)	309 (45)	
	3		31 (4)	74 (11)	135 (20)	217 (31)	12 (1)	54 (8)	113 (16)	190 (28)	
	4		9 (1)	94 (14)	137 (20)	217 (31)	8 (1)	81 (12)	117 (17)	191 (28)	
1.5 x 1.5 m	1		246 (36)	274 (40)	307 (44)	381 (55)	248 (36)	275 (40)	307 (44)	382 (55)	0.64 x 10 <sup>-1</sup> (2.51)
	2		-116 (-17)	-6 (-9)	72 (10)	231 (33)	-119 (-17)	-63 (-9)	71 (10)	230 (33)	
	3		-8 (-1)	46 (7)	109 (16)	179 (26)	-21 (-3)	32 (5)	94 (14)	160 (24)	
	4		101 (15)	90 (13)	114 (17)	179 (26)	96 (14)	81 (12)	101 (15)	160 (23)	
1 x 1 m	1		-	245 (36)	285 (41)	329 (48)	-	246 (36)	286 (41)	330 (49)	0.37 x 10 <sup>-1</sup> (1.46)
	2		-	-116 (-17)	-9 (-1)	134 (19)	-	-117 (-17)	-10 (-1)	133 (19)	
	3		-	-7 (-1)	76 (11)	136 (20)	-	-15 (-2)	66 (10)	125 (18)	
	4		-	100 (35)	93 (13)	136 (20)	-	96 (33)	86 (12)	126 (18)	

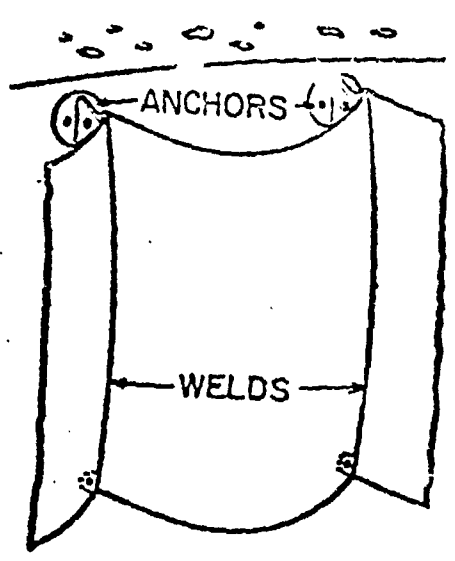
\*Locations 1 and 2 are the outside and inside surfaces of the shell at the support. Locations 3 and 4 are at the outside and inside surfaces of the shell at the center of the support pattern.



(a)



(b)



(c)

Figure 1. Joel G. Bennett and Charles A. Anderson

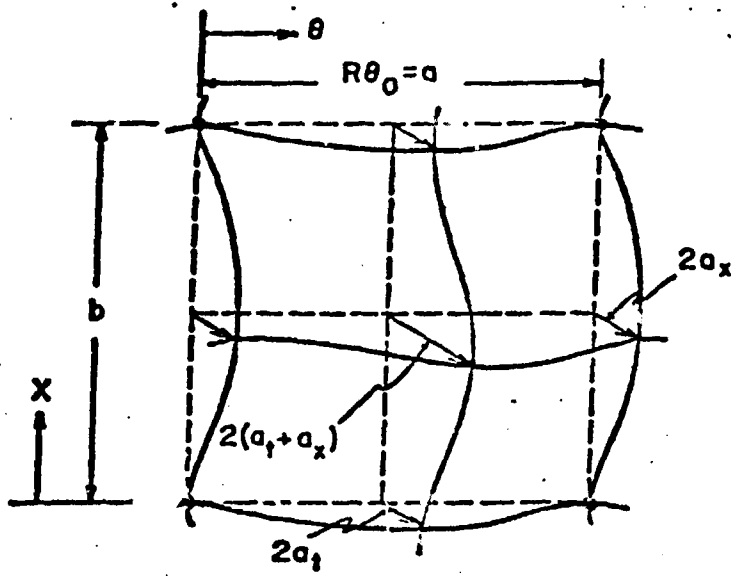


Figure 2.

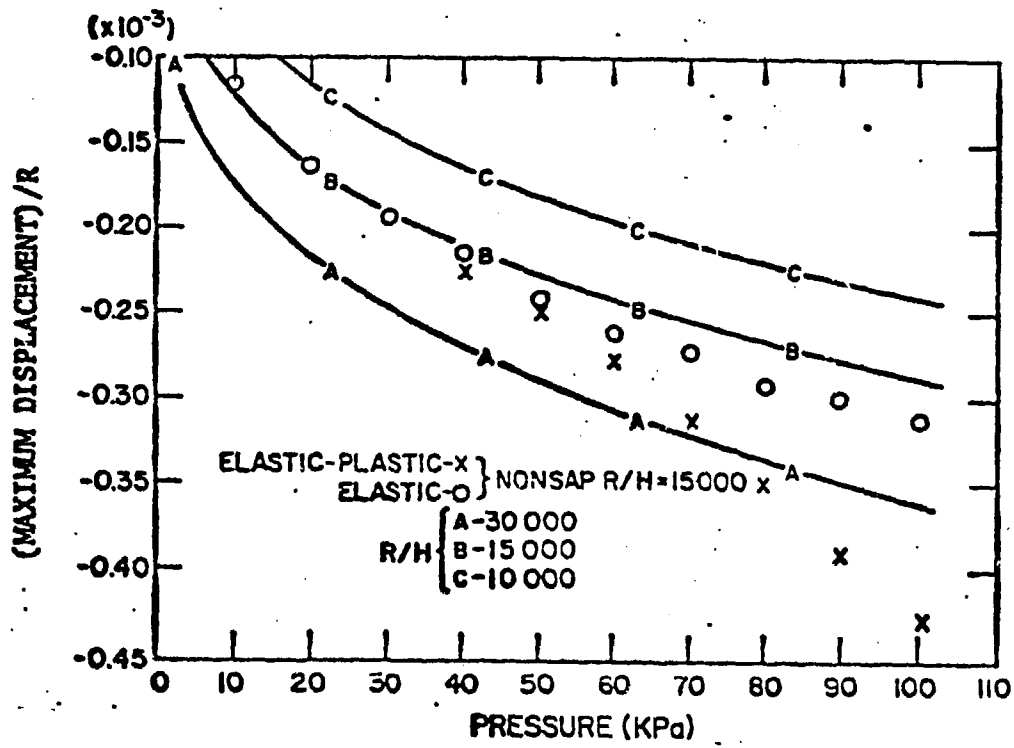


Figure 3. Joel G. Bennett and Charles A. Anderson

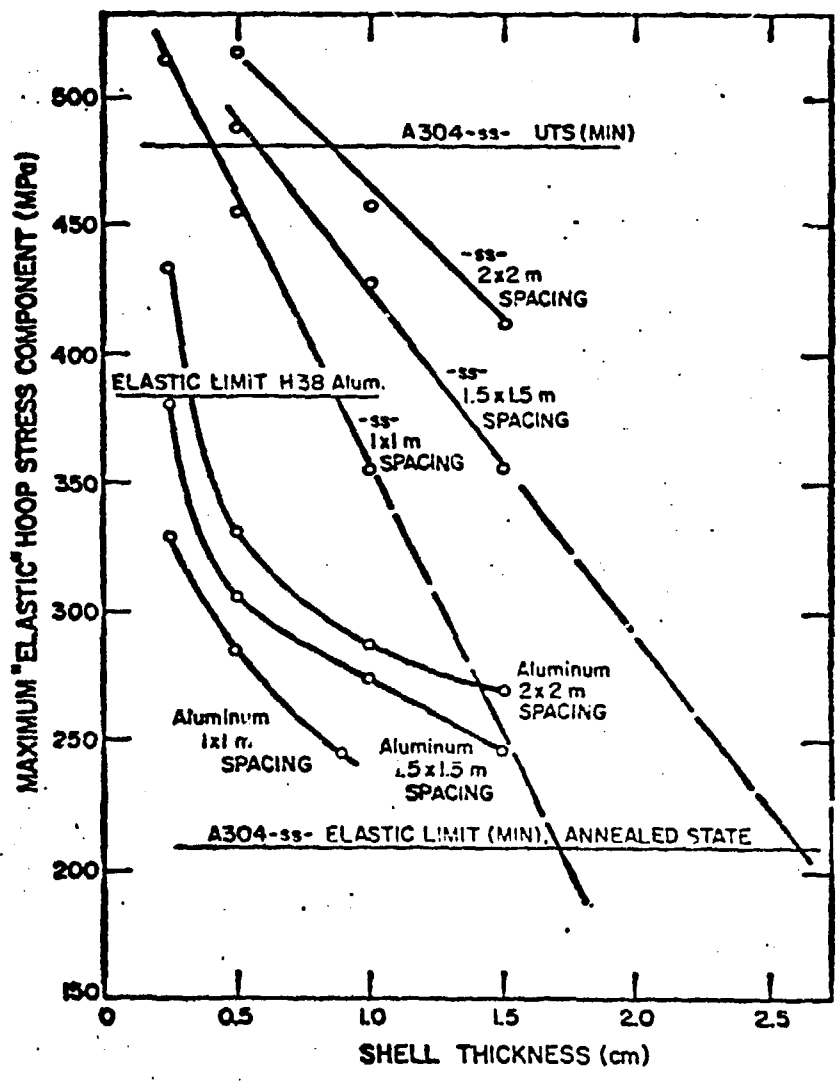


Figure 4. Joel G. Bennett and Charles A. Anderson

EFFECT OF -E- ON MAX STRESS A-2X2 B-1.5X1.5 C-1X1

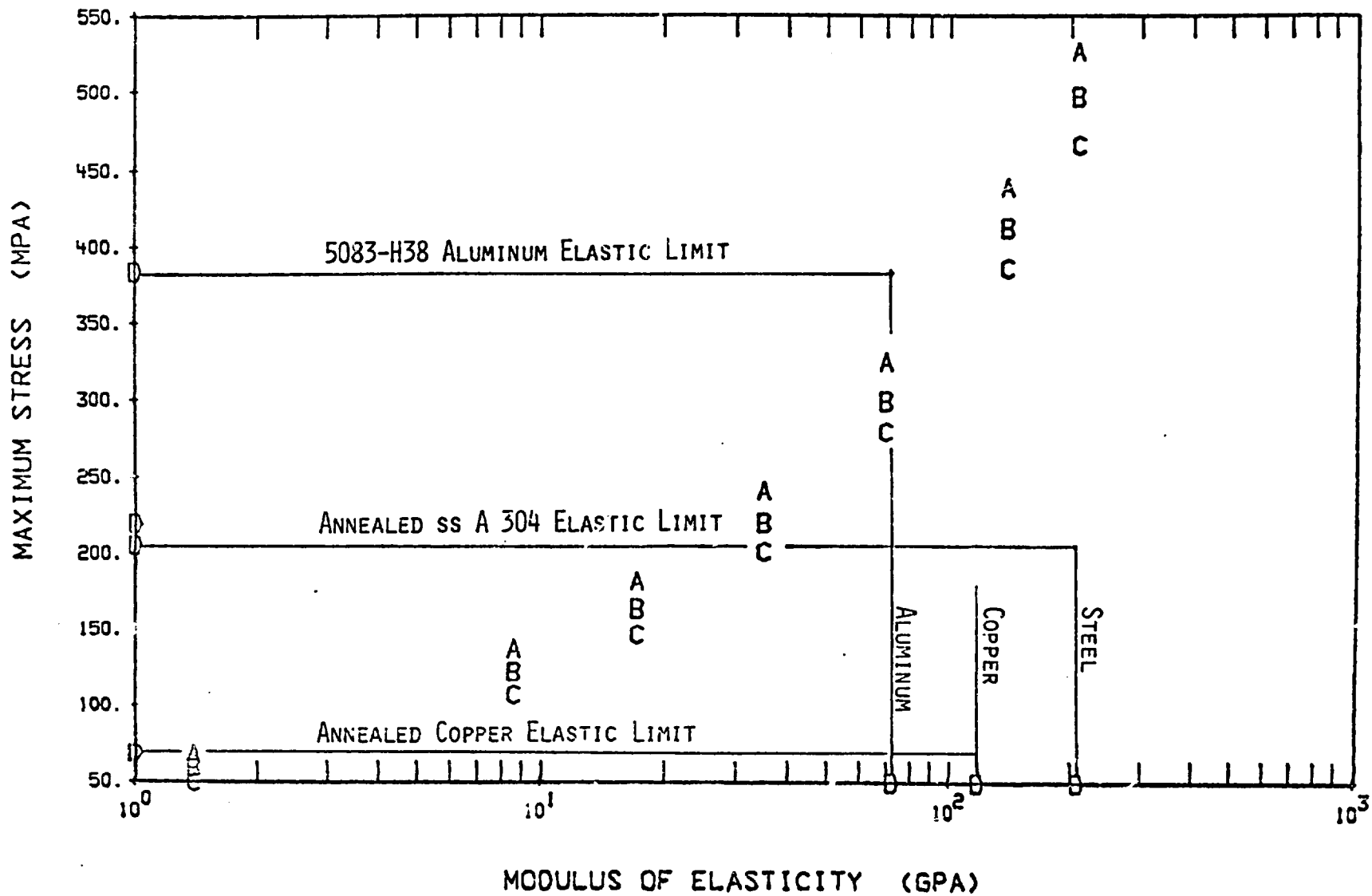


Figure 5. Joel G. Bennett and Charles A. Anderson

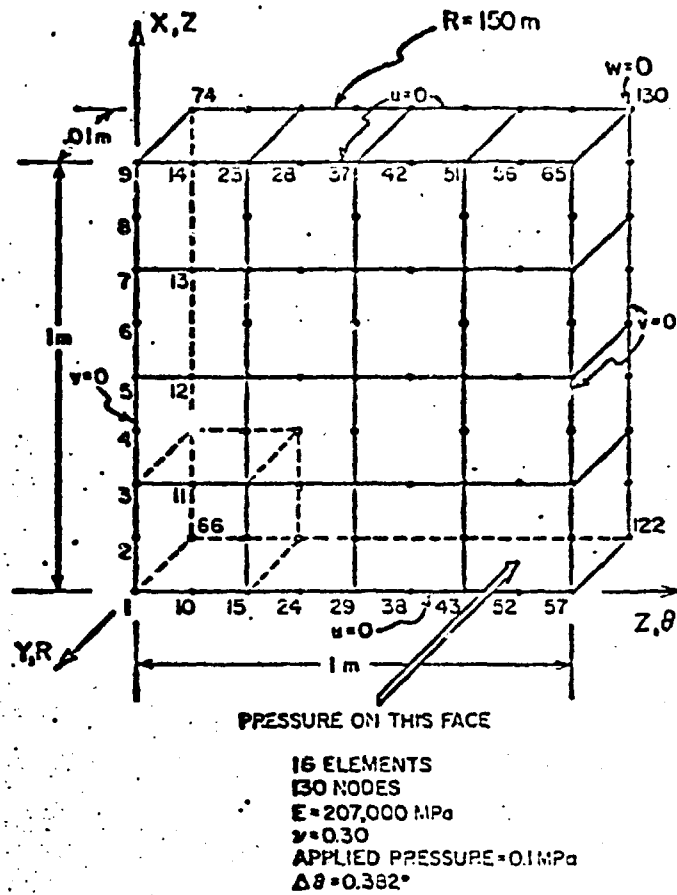


Figure 6.

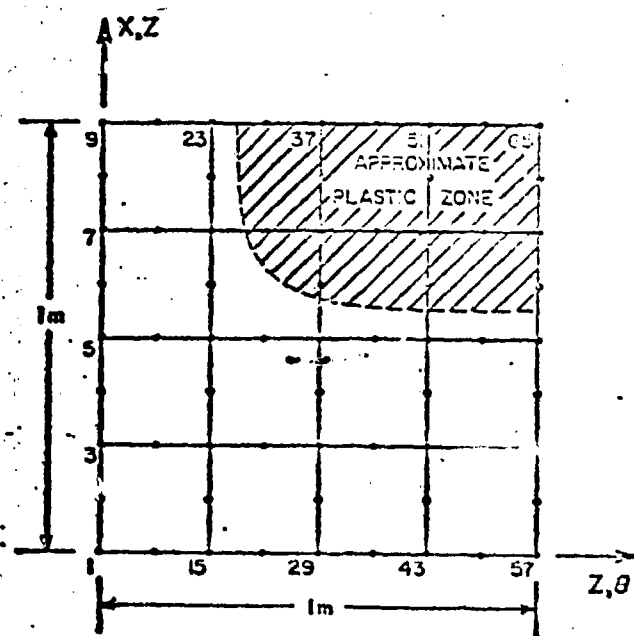


Figure 7. Joel G. Bennett and Charles A. Anderson

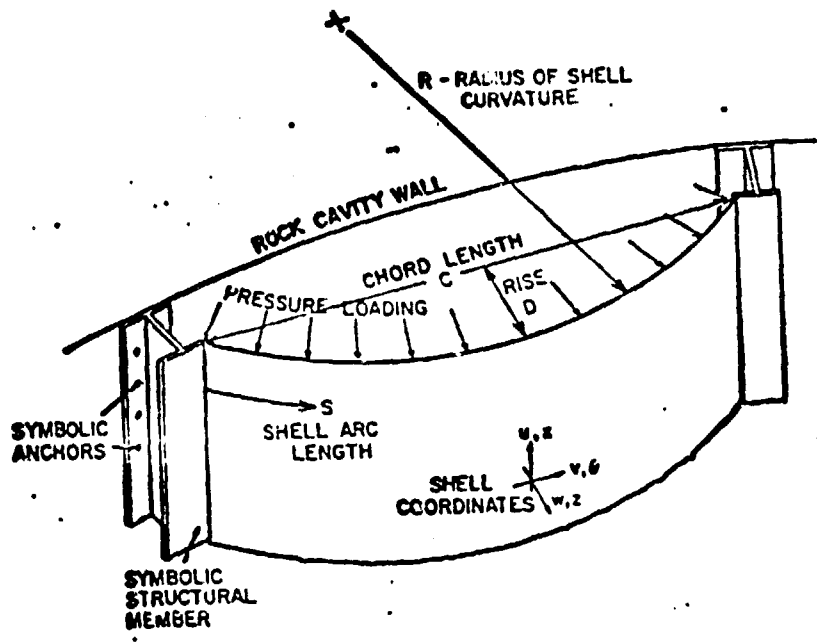


Figure 8.

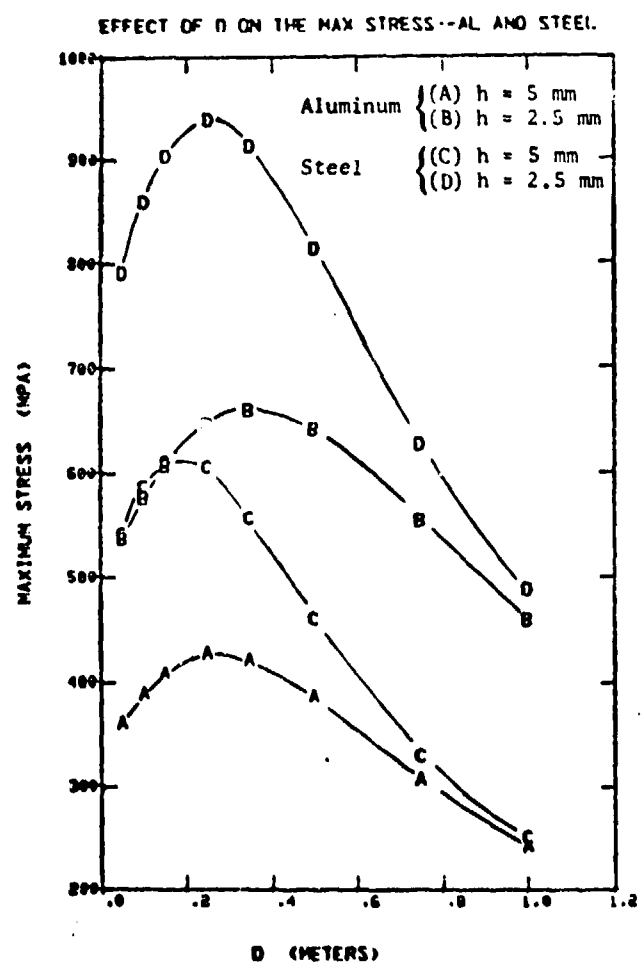


Figure 9. Joel G. Bennett and Charles A. Anderson